

# Optimization on a 3D Wing for Aerodynamic Lift using NACA 2412 Airfoil

J.Silambarasan<sup>1</sup> P.Tamilamudhan<sup>2</sup>

<sup>1</sup>P.G Scholar <sup>2</sup>Assistant Professor

<sup>1,2</sup>Department of Mechanical Engineering

<sup>1,2</sup>Sir ISSAC Newton Engineering and Technology, Nagapattinam

**Abstract**— The purpose of this project is to develop a procedure to numerically model airflow over wing using hypermesh and FLUENT. Three dimensional models for the airfoil 2412 were created, drawn and meshed in hypermesh using geometry data gathered by the National Advisory Committee for Aeronautics. Those models were read into FLUENT where boundary conditions flows were applied and the discretized Navier-Stokes equations were solved numerically. Numerical prediction of incompressible turbulent flow has been performed on a 3-D wing moving with a velocity of 50 m/s. CATIA, 3D modeling software was used to model 3D surface modeling of the wing. FLUENT, the computational fluid dynamics code, which incorporate k- $\epsilon$  turbulence model and segregated implicit solver was used to perform computation. The aerodynamic analysis was performed to study the flow behavior of the air over the wing. The analysis includes the contours of pressure and velocity that impacts the wing followed by an evaluation of the coefficient of lift.

**Key words:** Plane pin fin heat sink, Electronics cooling simulation, Pressure Drop, Thermal Resistance

## I. INTRODUCTION

Flight has been a major part of the world since it was first demonstrated by the Wright brothers in 1902. However, in depth studies into the effects of airflow over wings didn't occur until World War I (Anderson). In an attempt to better understand what made a good wing, the National Advisory Committee for Aeronautics, henceforth referred to as the NACA, was founded. In 1933 the NACA tested 78 airfoil shapes in their wind tunnels with the data being published in Technical Report No. 460, "The Characteristics of 78 Related Airfoil Sections from Tests in the Variable-Density Wind Tunnel." This report also resulted in the creation of the four-digit scheme for defining the basic geometry of the airfoil. This same naming scheme was then used to define the other airfoil families, such as the five-digit airfoils. In 1939 a low-turbulence two-dimensional wind tunnel was constructed for the sole purpose of airfoil testing (U.S. Centennial).

This report outlines the numeric procedure to analyze the NACA airfoil 2412 with a chord length of one meter and the Reynolds numbers of  $3 \times 10^6$ ,  $6 \times 10^6$ , and  $9 \times 10^6$ . Three dimensional model were created to compare FLUENT's accuracy in the two dimensional analysis and an actual sealed wing section three dimensional analysis.

The numerical process used for this airfoil will be used as a tutorial for student staking MAE 4440/7440, Aerodynamics, where they will be required to numerically analyze an airfoil of their own design. Once a procedure to replicate the NAC empirical data was found, an attempt to make a model showing the wingtip vortices phenomenon

was constructed. Unfortunately, a suitable mesh could not be found for the complicated airfoil geometry.

### A. LIFT:

A fluid flowing past the surface of a body exerts a force on it. Lift is the component of this force that is perpendicular to the oncoming flow direction. It contrasts with the drag force, which is

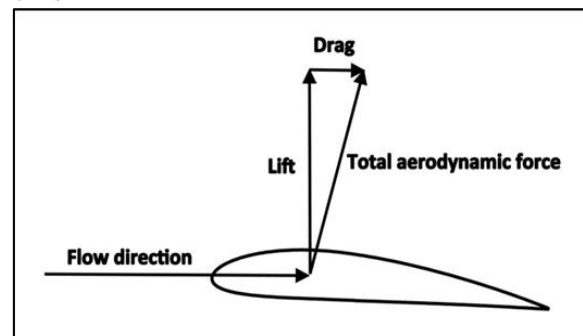


Fig 1: Flow deflection and newton's laws

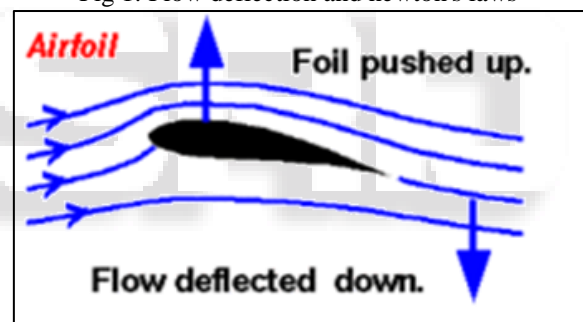


Fig. 1: (a) Airfoil

Newton's third law says that for every action there is an equal and opposite re-action. When an airfoil deflects air downwards, the air exerts an upward force on the airfoil. An airfoil generates lift by exerting a downward force on the air as it flows past. According to Newton's third law, the air must exert an equal and opposite (upward) force on the airfoil, which is the lift. In the case of an airplane wing, the wing exerts a downward force on the air and the air exerts an upward force on the wing. The air changes direction as it passes the airfoil and follows a path that is curved. Whenever airflow changes direction, a reaction force is generated opposite to the directional change. Newton's second law,  $F=ma$ , tells us that the lift force exerted on the air is equal to its mass times its downward acceleration. This is often more conveniently expressed as the rate of momentum change over time. The downward turning of the flow is not produced solely by the lower surface of the airfoil, and the flow following the upper surface contributes strongly to the downward-turning action. In some versions of this explanation, the tendency of the flow to follow the upper surface is referred to as the Coandă effect. This is a controversial usage of the term.

**B. Pressure Differences:**

Pressure is the normal force per unit area exerted by the air on itself and on surfaces that it touches. The lift force is transmitted through the pressure, which acts perpendicular to the surface of the airfoil. The air maintains physical contact at all points. Thus, the net force manifests itself as pressure differences. The direction of the net force implies that the average pressure on the upper surface of the airfoil is lower than the average pressure on the underside.

These pressure differences arise in conjunction with the curved air flow. Whenever a fluid follows a curved path, there is a pressure gradient perpendicular to the flow direction with higher pressure on the outside of curve and lower pressure on the inside. This direct relationship between curved streamlines and pressure differences was derived from Newton's second law by Leonhard Euler in 1754:

$$\frac{dp}{dR} = \rho \frac{v^2}{R}$$

The left hand side of this equation represents the pressure difference perpendicular to the fluid flow. On the right hand side  $\rho$  is the density,  $v$  is the velocity, and  $R$  is the radius of curvature. This formula shows that higher velocities and tighter curvatures create larger pressure differentials and that for straight flow ( $R \rightarrow \infty$ ) the pressure difference is zero.

**C. Lift Coefficient:**

If the lift coefficient for a wing at a specified angle of attack is known (or estimated using a method such as thin airfoil theory), then the lift produced for specific flow conditions can be determined using the following equation:<sup>[58]</sup>

$$L = \frac{1}{2} \rho v^2 A C_L$$

Where

- $L$  is lift force,
- $\rho$  is air density,
- $v$  is true airspeed,
- $A$  is planform area, and
- $C_L$  is the lift coefficient at the desired angle of attack, Mach number, and Reynolds number

**D. Lift of Three-Dimensional Wings:**

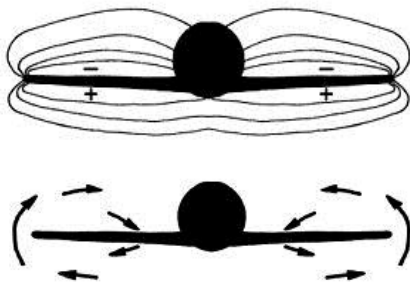


Fig. 2: Lift of Three-Dimensional Wings

Cross-section of an airplane wing-body combination showing velocity vectors of the three-dimensional lifting flow. For wings of moderate-to-high aspect ratio, the flow at any station along the span except close to the tips behaves much like flow around a two-dimensional airfoil, and most explanations of lift, like those above, concentrate on two-dimensional flow. However, even for wings of high aspect ratio, the three-dimensional effects associated with finite

span are significant across the whole span, not just close to the tips.

The lift tends to decrease in the span wise direction from root to tip, and the pressure distributions around the airfoil sections change accordingly in the span wise direction. Pressure distributions in planes perpendicular to the flight direction tend to look like the illustration at right. This span wise-varying pressure distribution is sustained by a mutual interaction with the velocity field. Flow below the wing is accelerated outboard, flow outboard of the tips is accelerated upward, and flow above the wing is accelerated inboard, which results in the flow pattern illustrated at right.

There is more downward turning of the flow than there would be in a two-dimensional flow with the same airfoil shape and sectional lift, and a higher sectional angle of attack is required to achieve the same lift compared to a two-dimensional flow. The wing is effectively flying in a downdraft of its own making, as if the free stream flow were tilted downward, with the result that the total aerodynamic force vector is tilted backward slightly compared to what it would be in two dimensions. The additional backward component of the force vector is called lift-induced drag.

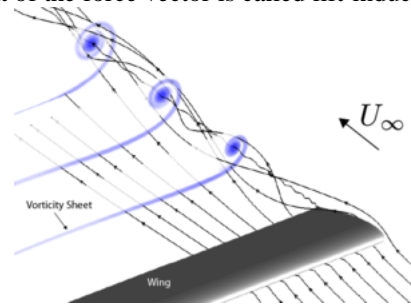
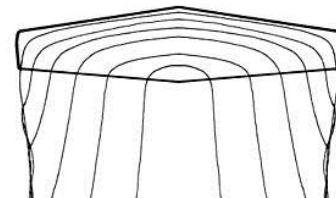


Fig. 3: Lift-Induced Drag

The difference in the spanwise component of velocity above and below the wing (between being in the inboard direction above and in the outboard direction below) persists at the trailing edge and into the wake downstream. After the flow leaves the trailing edge, this difference in velocity takes place across a relatively thin shear layer called a vortex sheet. As the vortex sheet is convected downstream from the trailing edge, it rolls up at its outer edges, eventually forming distinct wingtip vortices. The combination of the wingtip vortices and the vortex sheets feeding them is called the vortex wake.



In addition to the vorticity in the trailing vortex wake there is vorticity in the wing's boundary layer, which is often called the bound vorticity and which connects the trailing sheets from the two sides of the wing into a vortex system in the general form of a horseshoe. The horseshoe form of the vortex system was recognized by the British aeronautical pioneer Lanchester in 1907.

Given the distribution of bound vorticity and the vorticity in the wake, the Biot-Savart law (a vector-calculus relation) can be used to calculate the velocity perturbation anywhere in the field, caused by the lift on the wing.

Approximate theories for the lift distribution and lift-induced drag of three-dimensional wings are based on such analysis applied to the wing's horseshoe vortex system. In these theories, the bound vorticity is usually idealized and assumed to reside at the camber surface inside the wing.

Because the velocity is deduced from the vorticity in such theories, there is a tendency for some authors to describe the situation in terms that imply that the vorticity is the cause of the velocity perturbations, using terms such as "the velocity induced by the vortex," for example. But attributing causation to the vorticity in this way is not consistent with the physics. The real cause of the velocity perturbations is the pressure field.

#### E. Viscous Effects: Profile Drag and Stalling:

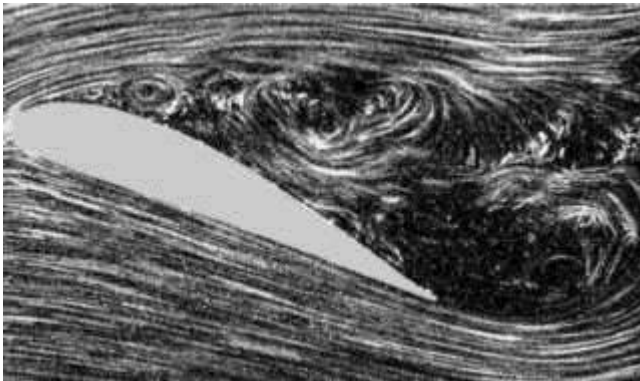


Fig. 3: Profile drag and stalling

No matter how smooth the surface of an airfoil seems, any real surface is rough on the scale of air molecules. Air molecules flying into the surface bounce off the rough surface in random directions not related to their incoming directions. The result is that when the air is viewed as if it were a continuous material, it is seen to be unable to slide along the surface, and the air's tangential velocity at the surface goes to practically zero, something known as the no-slip condition. Because the air at the surface has near-zero velocity and air away from the surface is moving, there is a thin boundary layer in which the air close to the surface is subjected to a shearing motion. The air's viscosity resists the shearing, giving rise to a shear stress at the airfoil's surface called skin-friction drag. Over most of the surface of most airfoils, the boundary layer is naturally turbulent, which increases skin-friction drag. Under usual flight conditions, the boundary layer remains attached to both the upper and lower surfaces all the way to the trailing edge, and its effect on the rest of the flow is modest. Compared to the predictions of inviscid-flow theory, in which there is no boundary layer, the attached boundary layer reduces the lift by a modest amount and modifies the pressure distribution somewhat, which results in a viscosity-related pressure drag over and above the skin-friction drag. The total of the skin-friction drag and the viscosity-related pressure drag is usually called the profile drag.

The maximum lift an airfoil can produce at a given airspeed is limited by boundary-layer separation. As the angle of attack is increased, a point is reached where the boundary layer can no longer remain attached to the upper surface. When the boundary layer separates, it leaves a region of recirculating flow above the upper surface, as illustrated in the flow-visualization photo at right. This is known as the *stall*, or *stalling*. At angles of attack above the

stall, lift is significantly reduced, though it is not zero. The maximum lift that can be achieved before stall, in terms of the lift coefficient, is generally less than 2.0 for single-element airfoils and can be more than 3.0 for airfoils with high-lift slotted flaps deployed.

#### F. Lift Forces on Bluff Bodies:

The flow around bluff bodies – i.e. without a streamlined shape, or stalling airfoils – may also generate lift, besides a strong drag force. This lift may be steady, or it may oscillate due to vortex shedding. Interaction of the object's flexibility with the vortex shedding may enhance the effects of fluctuating lift and cause vortex-induced vibrations. For instance, the flow around a circular cylinder generates a Kármán vortex street: vortices being shed in an alternating fashion from each side of the cylinder. The oscillatory nature of the flow is reflected in the fluctuating lift force on the cylinder, whereas the mean lift force is negligible. The lift force frequency is characterized by the dimensionless Strouhal number, which depends (among others) on the Reynolds number of the flow.

For a flexible structure, this oscillatory lift force may induce vortex-induced vibrations. Under certain conditions – for instance resonance or strong spanwise correlation of the lift force – the resulting motion of the structure due to the lift fluctuations may be strongly enhanced. Such vibrations may pose problems and threaten collapse in tall man-made structures like industrial chimneys.

In the Magnus effect, a lift force is generated by a spinning cylinder in a freestream. Here the mechanical rotation acts on the boundary layer, causing it to separate at different locations on the two sides of the cylinder. The asymmetric separation changes the effective shape of the cylinder as far as the flow is concerned such that the cylinder acts like a lifting airfoil with circulation in the outer flow.

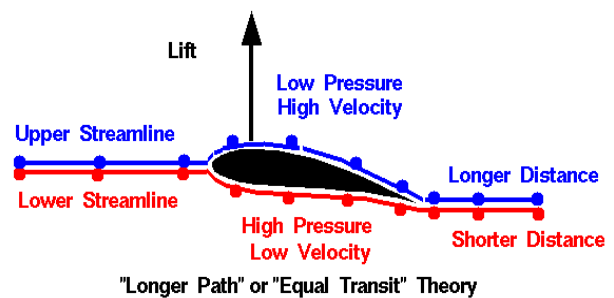


Fig. 4: Lift forces on bluff bodies

#### G. DRAG:

In fluid dynamics, drag (sometimes called air resistance, a type of friction, or fluid resistance, another type of friction or fluid friction) refers to forces acting opposite to the relative motion of any object moving with respect to a surrounding fluid. This can exist between two fluid layers (or surfaces) or a fluid and a solid surface. Unlike other resistive forces, such as dry friction, which are nearly independent of velocity, drag forces depend on velocity. Drag force is proportional to the velocity for a laminar flow and for a squared velocity for a turbulent flow. Even though the ultimate cause of a drag is viscous friction, the turbulent drag is independent of viscosity. Drag forces

always decrease fluid velocity relative to the solid object in the fluid's path.

## II. DRAG IN AERODYNAMICS

### A. Lift-Induced Drag:

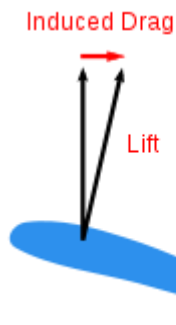


Fig. 5: Lift-Induced Drag

Lift-induced drag (also called induced drag) is drag which occurs as the result of the creation of lift on a three-dimensional lifting body, such as the wing or fuselage of an airplane. Induced drag consists of two primary components, including drag due to the creation of vortices (vortex drag) and the presence of additional viscous drag (lift-induced viscous drag). The vortices in the flow-field, present in the wake of a lifting body, derive from the turbulent mixing of air of varying pressure on the upper and lower surfaces of the body, which is a necessary condition for the creation of lift. With other parameters remaining the same, as the lift generated by a body increases, so does the lift-induced drag. For an aircraft in flight, this means that as the angle of attack, and therefore the lift coefficient increases to the point of stall, so does the lift-induced drag. At the onset of stall, lift is abruptly decreased, as is lift-induced drag, but viscous pressure drag, a component of parasite drag, and increases due to the formation of turbulent unattached flow on the surface of the body.

### B. Parasitic Drag:

Parasitic drag (also called parasite drag) is drag caused by moving a solid object through a fluid. Parasitic drag is made up of multiple components including viscous pressure drag (form drag), and drag due to surface roughness (skin friction drag). Additionally, the presence of multiple bodies in relative proximity may incur so called interference drag, which is sometimes described as a component of parasitic drag.

In aviation, induced drag tends to be greater at lower speeds because a high angle of attack is required to maintain lift, creating more drag. However, as speed increases the induced drag becomes much less, but parasitic drag increases because the fluid is flowing more quickly around protruding objects increasing friction or drag. At even higher speeds in the transonic, wave drag enters the picture. Each of these forms of drag changes in proportion to the others based on speed. The combined overall drag curve therefore shows a minimum at some airspeed - an aircraft flying at this speed will be at or close to its optimal efficiency. Pilots will use this speed to maximize endurance (minimum fuel consumption), or maximize gliding range in the event of an engine failure.

### C. Power Curve in Aviation:

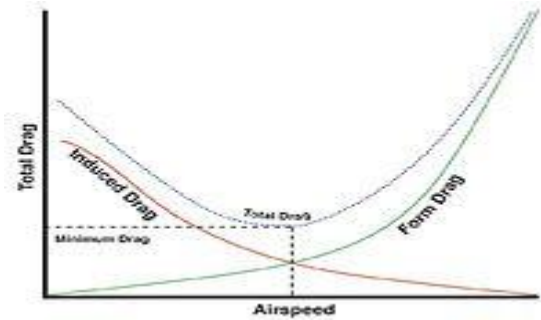


Fig. 6: Power curve in aviation

The interaction of parasitic and induced drag vs. airspeed can be plotted as a characteristic curve, illustrated here. In aviation, this is often referred to as the power curve, and is important to pilots because it shows that, below a certain airspeed, maintaining airspeed counter intuitively requires more thrust as speed decreases, rather than less. The consequences of being "behind the curve" in flight are important and are taught as part of pilot training. At the subsonic airspeeds where the "U" shape of this curve is significant, wave drag has not yet become a factor, and so it is not shown in the curve.

### D. Wave Drag in Transonic and Supersonic Flow:

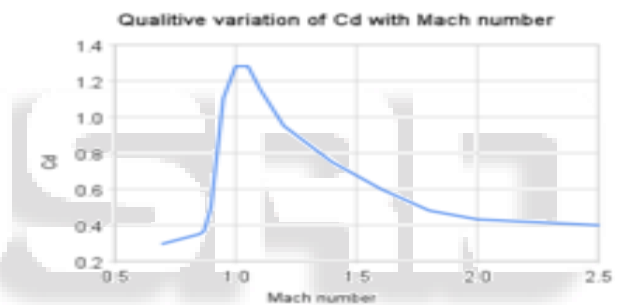


Fig. 7: Wave drag in transonic and supersonic flow

Wave drag (also called compressibility drag) is drag which is created by the presence of a body moving at high speed through a compressible fluid. In aerodynamics, Wave drag consists of multiple components depending on the speed regime of the flight.

In transonic flight (Mach numbers greater than about 0.8 and less than about 1.4), wave drag is the result of the formation of shockwaves on the body, formed when areas of local supersonic (Mach number greater than 1.0) flow are created. In practice, supersonic flow occurs on bodies traveling well below the speed of sound, as the local speed of air on a body increases when it accelerates over the body, in this case above Mach 1.0. However, full supersonic flow over the vehicle will not develop until well past Mach 1.0. Aircraft flying at transonic speed often incur wave drag through the normal course of operation. In transonic flight, wave drag is commonly referred to as transonic compressibility drag. Transonic compressibility drag increases significantly as the speed of flight increases towards Mach 1.0, dominating other forms of drag at these speeds.

In supersonic flight (Mach numbers greater than 1.0), wave drag is the result of shockwaves present on the body, typically oblique shockwaves formed at the leading and trailing edges of the body. In highly supersonic flows, or in bodies with turning angles sufficiently

large, unattached shockwaves, or bow waves will instead form. Additionally, local areas of transonic flow behind the initial shockwave may occur at lower supersonic speeds, and can lead to the development of additional, smaller shockwaves present on the surfaces of other lifting bodies, similar to those found in transonic flows. In supersonic flow regimes, wave drag is commonly separated into two components, supersonic lift-dependent wave drag and supersonic volume-dependent wave drag.

The closed form solution for the minimum wave drag of a body of revolution with a fixed length was found by Sears and Haack, and is known as the Sears-Haack Distribution. Similarly, for a fixed volume, the shape for minimum wave drag is the Von Karman Ogive. Busemann's Biplane is not, in principle, subject to wave drag at all when operated at its design speed, but is incapable of generating lift.

**E. CFD:**

Computational Fluid Dynamics (CFD) is the science of predicting fluid flow, heat transfer, mass transfer, chemical reactions, and related phenomena by solving mathematical equations that represent physical laws, using a numerical process.

- Conservation of mass, momentum, energy, species
- The result of CFD analyses is relevant engineering data
- Conceptual studies of new design
- Detailed product development
- Troubleshooting
- Redesign
- CFD analysis complements testing and experimentation.
- Reduces the total effort required in the laboratory.

**F. Flow Chart:**

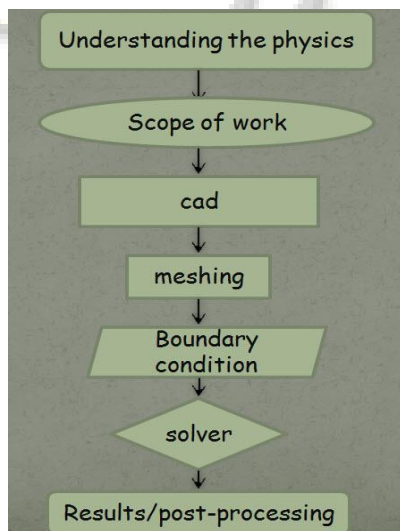


Fig. 8: Flow Chart

**III. REPORTS**

The computation is performed using the finite-volume technique with upwind discretization to solve the two-dimensional compressible RANS equations. The air is considered to be a calorically perfect gas with constant ratio of specific heat. The space discretization is performed by a cell-centered formulation. To account for the directed

propagation of information in the inviscid part of the equations, the advection upstream splitting method flux vector splitting is applied for the approximation of the convective flux functions. Higher-order accuracy for the upwind discretization and consistency with the central differences used for the diffusive term is achieved by the monotonic upstream scheme for conservation laws extrapolations. Time integration is performed by an explicit five stage Runge-Kutta time-stepping scheme. To enhance convergence, a multi-grid method, implicit residuals smoothing, and local time stepping are applied.

**A. Four-Digit Airfoils:**

All the airfoils in the NACA four-digit airfoil family are defined by a series of four numerical digits, i.e. 2412. The first digit is the maximum value of the mean line in hundredths of the chord and is represented in the following equations with the letter *m*. The second number represents the position on the chord of the maximum mean line in tenths of the chord and is represented with the letter *p*. The last two numbers designate the maximum thickness of the airfoil in hundredths of the chord and are represented by *t*. Therefore, the airfoil 2412 tells us that the airfoil has a maximum mean line value of two hundredths of the chord length at a position four tenths the chord from the front of the airfoil and a maximum thickness of twelve hundredths the chord length, see figure 6.



Fig. 9: Diagram displaying the chord length, maximum chamber, position of max chamber and max thickness of the airfoil geometry

**B. CATIA:**

CATIA is modeling software that is capable of creating meshed geometries that can be read into FLUENT and other analysis software. An outline for the CATIA geometry creation process can be seen in figure 8.

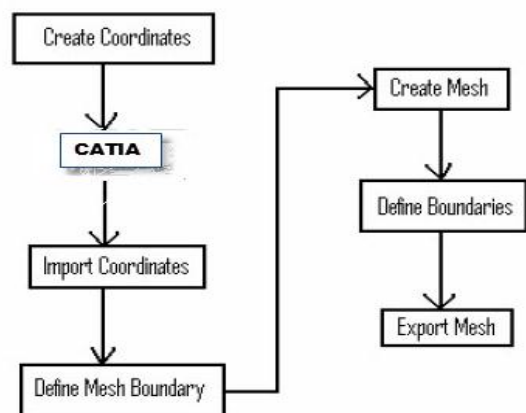


Fig. 10: CATIA

**C. Coordinate Format:**

Since the airfoil geometry is defined by sets of coordinate points, the more points defined will increase the accuracy of

the model. An airfoil geometry defined by one hundred points for both the top and bottom surface will result in a good definition. The list of coordinates seen in figure 2 were derived by scripting equations 1-6 into a Matlab M-file, which can be found in the Appendix, which then supplied the corresponding x, y, and z coordinate for each of the hundred points along the upper and lower surface of the airfoil. With the coordinates defined, they must be listed in a text document in the following format:

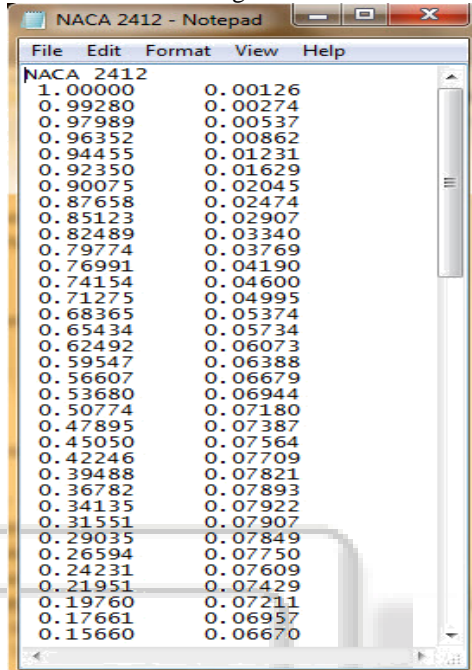


Fig. 11: Proper coordinate format for reading coordinates into CATIA

The top two numbers, 100 and 2, tell Gambit that it is going to read in two sets of one hundred coordinates one right after the other. The column on the left is the x coordinates. The central column is the y-coordinates and the right column is the z coordinates. There must be no empty lines between the rows of coordinates and at least one space separating the columns of coordinates from one another. The coordinates should also be listed vertically moving from the nose of the airfoil toward the tail for the upper surface first and then the lower surface. A note of interest, by using equations 1-6, the two coordinates that define the tail of the airfoil do not bring the geometry to a single point.

#### D. Creating the Airfoil Geometry:

Launch Gambit. Once CATIA is open make certain the solver is set for the appropriate output, i.e. fluent 5/6, by selecting solver → fluent 5/6. The coordinate document must now be imported into CATIA.



Fig. 12: Imported airfoil geometry

#### E. Creating the WING Geometry:

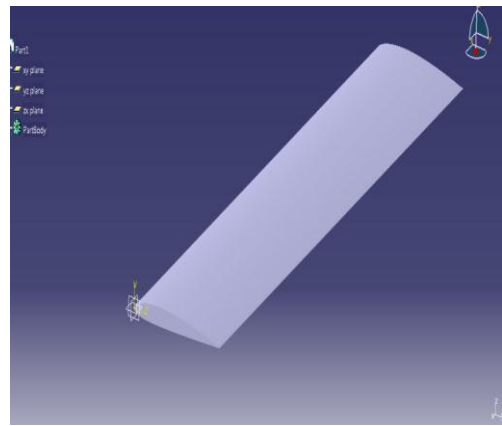


Fig. 13: Wing geometry

#### F. Meshing and Reading Mesh Components:

- Components are defined in pre-processor
- Cell = control volume into which domain is broken up
- Computational domain is defined by mesh that represents the fluid and solid regions of interest.
- Face = boundary of a cell Edge = boundary of a face
- Node = grid point
- Zone = grouping of nodes, faces, and/or cells

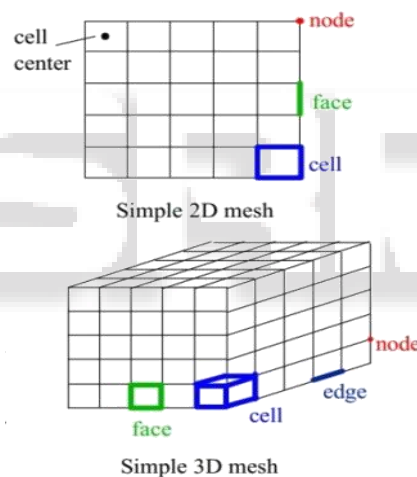


Fig. 14: Meshes description

#### IV. CONCLUSION

The main objective to estimate the lift coefficient and flow visualization is achieved. Aerodynamics lift for the NACA 2412 is 0.219 at ranging velocity between 50m/s. The analysis shows aerodynamics lift in term of forces or lift coefficient proportionally increased to the square of velocity. The contour plot of velocity and pressure were shown the in aerodynamics lift analysis as a visualization analysis. The pattern of visualization for every velocity depict quite same either for velocity contour plot or pressure contour plot. Here my project doesn't end and the optimization of NACA 2412 is to be continued in the project (phase-2). The lift in the current wing is 0.219 and the drag is 0.002. There are different techniques to increase the lift the one way is changing the co-ordinates according to aerodynamic considerations.

REFERENCES

- [1] Abbott, I., and Von Doenhoff, A., 1959, Theory of Wing Sections, Dover, Mineola, NY
- [2] Anderson, Jr., J., 2001, Fundamentals of Aerodynamics, 3rd Ed., McGraw Hill, Singapore
- [3] Eastman, J., and Ward, K., 1933, "The characteristics of 78 related airfoil sections from tests in the variable-density wind tunnel," NACA-report-460
- [4] Aerospaceweb.org, "NACA Airfoil Series," <http://www.aerospaceweb.org/question/airfoils/q0041.shtml> (2006)
- [5] FLUENT, "studentFLUENT - Tutorial Library - Airfoil," [http://www.FLUENT.com/software/studentFLUENT/tutorial\\_airfoil.htm](http://www.FLUENT.com/software/studentFLUENT/tutorial_airfoil.htm) (16 Nov 2006)
- [6] U.S. Centennial Flight Commission, "The National Advisory Committee for Aeronautics (NACA),"
- [7] Mellen, C., Fröhlich, J., and Rodi, W., 2003, "Lessons from LESFOIL Project on Large-Eddy Simulation of Flow Around an Airfoil," AIAA Journal, Vol. 41, No. 4.

